



## Stabilization of Ferromagnetic Metallic Phase and Anomalous Magnetotransport in $\text{Pr}_{1-X}\text{Ca}_X(\text{Mn}_{1-Z}\text{Co}_Z)\text{O}_3$

Manabu IKEBE, Hiroyuki FUJISHIRO, Hajime YAMAZAKI and Shingo KANOH

*Faculty of Engineering, Iwate University, Morioka 020-8551, Japan*

The magnetization  $M(T)$  and the electrical resistivity  $\rho(T)$  of  $\text{Pr}_{1-X}\text{Ca}_X(\text{Mn}_{1-Z}\text{Co}_Z)\text{O}_3$  were measured and the magnetic and the electronic phase diagram of this system was determined as a function of Ca and Co concentrations and the magnetic fields. For  $0.30 \leq X \leq 0.55$ , where the charge and orbital ordered phase is the ground state in the  $Z=0$  system, the ferromagnetic metallic (FM-M) state is materialized by the Co substitution and the  $T_c$ - $X$  curves take a maximum around  $X=0.4\sim 0.45$ . The results were compared with those of the Cr- and Ni-doped systems.

KEYWORDS:  $\text{Pr}_{1-X}\text{Ca}_X(\text{Mn}_{1-Z}\text{Co}_Z)\text{O}_3$ , phase diagram, charge and orbital ordering, ferromagnetic transition

### §1. Introduction

The perovskite-type manganites,  $\text{RE}_{1-X}\text{AE}_X\text{MnO}_3$  (RE: rare-earth elements, AE: alkaline-earth elements), have been extensively studied from both physical and applicational interests in the colossal magnetoresistance (CMR) effect.<sup>1,2</sup> In small (RE,AE) ions such as RE=Pr, Nd and AE=Ca, the  $\text{MnO}_6$  network is structurally distorted and the  $e_g$  electron transfer between Mn ion sites is hindered. Then the small (RE,AE) ions tend to suppress the double exchange (DE) interaction and the other competitive effects such as the superexchange interaction or the enhanced electron-phonon coupling through the Jahn-Teller (J-T) effect become more important to control the physical properties. In the  $\text{Pr}_{1-X}\text{Ca}_X\text{MnO}_3$  (PCMO) system, the so-called CE-type charge/orbital order (CO/OO) is realized over a wide Ca concentration  $X$  ( $0.30 \leq X \leq 0.75$ ).<sup>3</sup> By the substitution for the Mn site by other transition metals such as Co and Cr, the CO/OO state is destroyed and the ferromagnetic metal (FM-M) state is induced.<sup>4,5</sup> Although the substitution effect of the Cr ions for the Mn site has been rather widely investigated, the Co concentration dependence of the phase diagram for the manganite systems has not been so systematically investigated.

In the present paper, we report the magnetization  $M(T)$  and electrical resistivity  $\rho(T)$  of  $\text{Pr}_{1-X}\text{Ca}_X(\text{Mn}_{1-Z}\text{Co}_Z)\text{O}_3$  system for various Ca and Co concentrations under the applied fields. The magnetic and electronic phase diagram of this system was determined at 0 T and 5 T. By comparing the Cr- and Ni-doped PCMO systems, we try to make clear how does the FM-M phase compete with the CO/OO phase in this small A-site ion system.

### §2. Experimental

The  $\text{Pr}_{1-X}\text{Ca}_X(\text{Mn}_{1-Z}\text{Co}_Z)\text{O}_3$  ( $0.20 \leq X \leq 0.80$ ,  $Z \leq 0.10$ ) crystals were prepared from stoichiometric mixtures of  $\text{Pr}_6\text{O}_{11}$ ,  $\text{CaCO}_3$ ,  $\text{Mn}_3\text{O}_4$  and  $\text{CoO}$  powders.<sup>6</sup> The mixtures were calcined twice at  $1000^\circ\text{C}$  for 24 h in air, pressed into pellets and then sintered at  $1500^\circ\text{C}$  for 8

h in air. Also the Cr- and Ni-doped samples were similarly prepared. The measured densities of each sample are about 85% of the ideal one. The X-ray diffraction analyses confirmed that all the substituted samples were a single orthorhombic phase. The electrical resistivity  $\rho(T)$  was measured by a standard four-terminal method, using a Gifford-McMahon (GM) cycle helium refrigerator as a cryostat. The magnetic field up to 5 T was applied by a cryocooler-cooled superconducting magnet in the perpendicular direction to the current flow. The magnetization  $M(T)$  was measured using a SQUID magnetometer under a magnetic field of 0.5 T after the process of zero field cooling (ZFC).

### §3. Results and Discussion

Figure 1 shows the temperature dependence of  $\rho(T)$  of  $\text{Pr}_{1-X}\text{Ca}_X(\text{Mn}_{1-Z}\text{Co}_Z)\text{O}_3$  ( $X=0.45$  and  $0.50$ ) samples for various  $Z$ . The zero-field resistivity  $\rho(T)$  of the  $Z=0$  sample shows an abrupt upturn just below the CO/OO temperature  $T_{\text{CO}}=235$  K and then monotonically increases with decreasing temperature. In the applied field of 5 T,  $T_{\text{CO}}$  decreases to  $\sim 225$  K and  $\rho(T)$  shows nearly

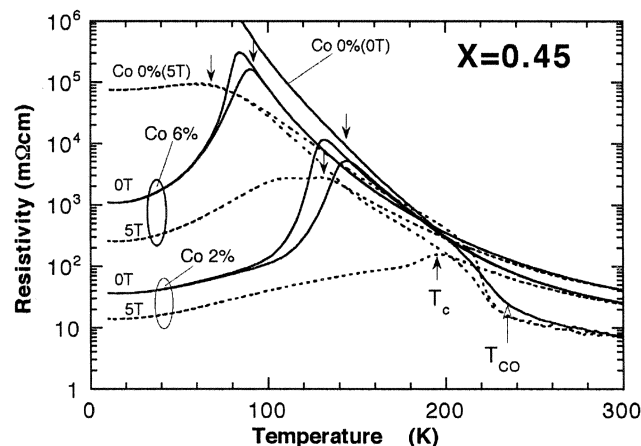


Fig.1. The temperature dependence of the electrical resistivity  $\rho(T)$  of  $\text{Pr}_{0.55}\text{Ca}_{0.45}(\text{Mn}_{1-Z}\text{Co}_Z)\text{O}_3$  for various  $Z$  with and without applied field of 5 T.

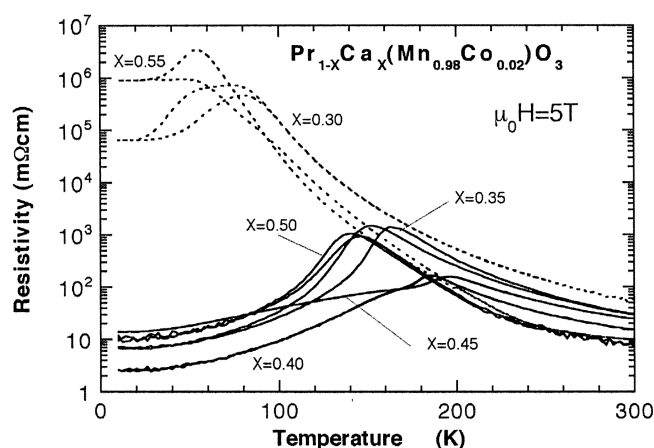


Fig. 2. The resistivity  $\rho(T)$  of  $\text{Pr}_{1-x}\text{Ca}_x(\text{Mn}_{0.98}\text{Co}_{0.02})\text{O}_3$  samples ( $0.30 \leq x \leq 0.55$ ) for the fixed Co content of  $Z=0.02$  under the magnetic field of 5 T.

temperature independent behavior below  $T=70$  K, which may suggest the partial destruction of the CO/OO state in this temperature range. For the  $Z=0.02$  sample, the zero-field  $\rho(T)$  shows a drastic reduction at  $T_c=150$  K and 160 K on cooling and heating runs, respectively, and  $\rho(T)$  behaves metallic below  $T_c$ . This hysteretic  $\rho(T)$  behavior indicates that the transition to the FM-M phase (from the CO/OO phase) is of the first order. Under the magnetic field of 5 T,  $\rho(T)$  decreases and  $T_c$  increases, while the hysteresis of  $\rho(T)$  is wiped out. This result suggests that, in the field of 5 T,  $T_c(5\text{ T})=195$  K has completely exceeded  $T_{CO}(5\text{ T})$ . For the  $Z=0.06$  sample,  $\rho(T)$  increases and  $T_c$  decreases compared with those for  $Z=0.02$ . The hysteresis in  $\rho(T)$  is absent. For  $Z=0.10$ , the  $\rho(T)$  drop cannot be seen even in the applied field of 5 T. These results indicate that the Co substitution drastically destroys the CO/OO state but it deteriorates the FM-M phase as well. Because the  $M(T)$  measurement on our FM insulating (FM-I) samples ( $x \leq 0.30$ ), where the FM superexchange interaction is dominant, confirmed that  $T_c$  remains nearly constant up to  $Z=0.10$ , the deteriorating effect on the FM-M phase may come mainly from the suppression of the DE interaction caused by the increased  $e_g$  electron scattering by Co impurities.

Figure 2 shows the electrical resistivity  $\rho(T)$  of  $\text{Pr}_{1-x}\text{Ca}_x(\text{Mn}_{0.98}\text{Co}_{0.02})\text{O}_3$  samples ( $0.30 \leq x \leq 0.55$ ) for a fixed Co content of  $Z=0.02$  under the magnetic field of 5 T. For  $x=0.30$ , the insulator-metal (I-M) transition is barely observable below 80 K together with hysteresis. For the  $0.35 \leq x \leq 0.50$  samples, the I-M transition clearly occurs at  $T_c$ .  $T_c$  increases with increasing  $x$  and reaches a maximum at 190 K for  $x=0.45$  and then decreases for  $x=0.50$ . For  $x=0.55$ , the I-M transition similar to that of  $x=0.30$  is again barely observable.  $T_c$  against  $x$  in zero magnetic field behaves similarly to that in 5 T, but  $T_c$  maximum occurs at a slightly lower  $x$  value.

Figure 3 shows the temperature dependence of the magnetization  $M(T)$  of the  $\text{Pr}_{1-x}\text{Ca}_x(\text{Mn}_{0.98}\text{Co}_{0.02})\text{O}_3$  ( $0.25 \leq x \leq 0.55$ ) under the magnetic field of 0.5 T. For the  $x=0.25$  and 0.30 samples, FM state is observed below  $T_c=130$  K, but the  $\rho(T)$  is that of an insulator (FM-I). For the  $x=0.35$  sample, the abrupt  $M(T)$  upturn at 90 K

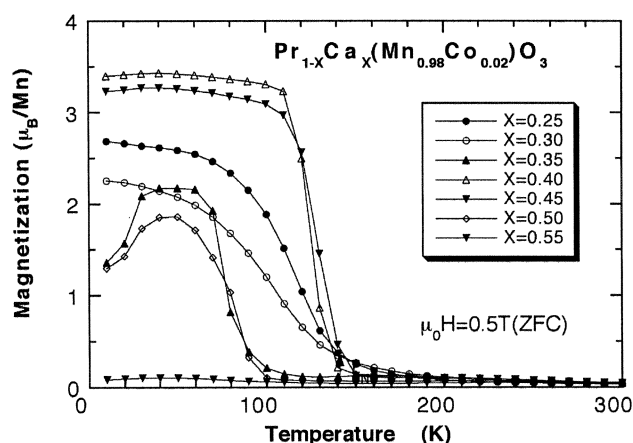


Fig. 3. The temperature dependence of the magnetization  $M(T)$  of  $\text{Pr}_{1-x}\text{Ca}_x(\text{Mn}_{0.98}\text{Co}_{0.02})\text{O}_3$  samples ( $0.25 \leq x \leq 0.55$ ) under the magnetic field of 0.5 T after ZFC.

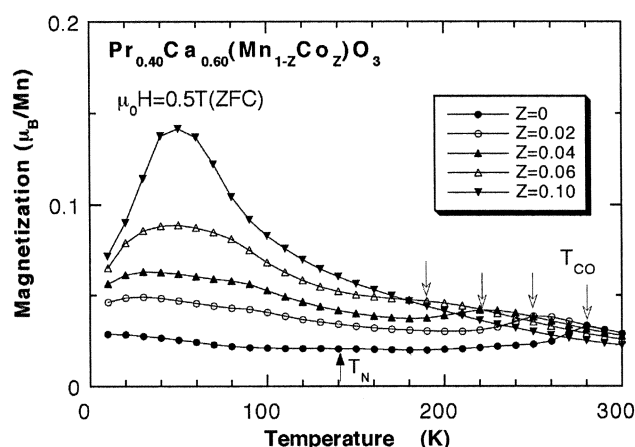


Fig. 4. The magnetization  $M(T)$  of the  $\text{Pr}_{0.40}\text{Ca}_{0.60}(\text{Mn}_{1-z}\text{Co}_z)\text{O}_3$  samples ( $0 \leq z \leq 0.10$ ) as a function of temperature  $T$ .

is consistent with the first-order transition. The abrupt  $M(T)$  upturn appears also for  $x=0.40$ , 0.45 and 0.50 samples. It is to be noticed that  $T_c$  estimated from the upturn of  $M(T)$  has a gap between the FM-I ( $x=0.30$ ) and FM-M ( $x=0.35$ ) phases.

Figure 4 shows the magnetization  $M(T)$  of the  $\text{Pr}_{0.40}\text{Ca}_{0.60}(\text{Mn}_{1-z}\text{Co}_z)\text{O}_3$  samples ( $0 \leq z \leq 0.10$ ). For  $x \geq 0.60$ , the FM-M state is not stabilized by the Co substitution, nor by the applied field up to 5 T. Although the anomaly of resistivity around  $T_{CO}$  is not clear for the Co substituted samples, the decrease in  $M(T)$  is clearly observable and we can locate  $T_{CO}$  by the local maximum of the  $M(T)$  shown by the arrows in this figure.  $T_{CO}$  monotonically decreases with increasing  $Z$ .

Figures 5(a) and 5(b) present the magnetic and electronic phase diagram of  $\text{Pr}_{1-x}\text{Ca}_x(\text{Mn}_{1-z}\text{Co}_z)\text{O}_3$  system under the magnetic fields of 0 T and 5 T, respectively. In Fig. 5(a),  $T_c$ ,  $T_{CO}$  and the Neel temperature  $T_N$  for the  $Z=0$  samples were determined by the  $M(T)$  measurement (0.5 T after ZFC). For the Co-substituted samples,  $T_c$  was determined from the resistivity  $\rho(T)$  anomaly in the heating run and  $T_{CO}$  was determined from the  $M(T)$  anomaly (0.5 T in ZFC). In Fig. 5(b), both  $T_c$  and  $T_{CO}$  at 5 T were determined from the  $\rho(T)$

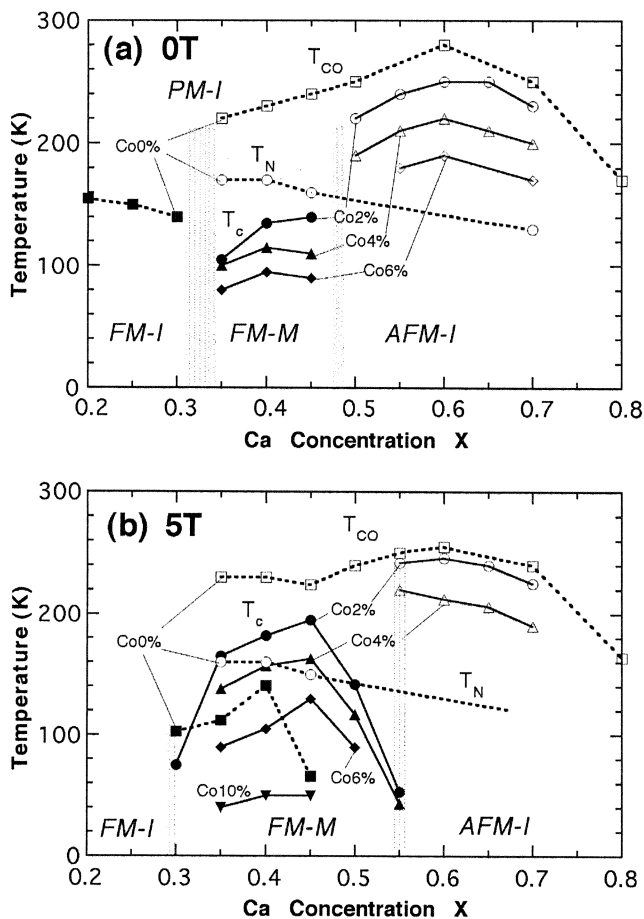


Fig. 5. Proposed magnetic and electronic phase diagram of  $\text{Pr}_{1-x}\text{Ca}_x(\text{Mn}_{1-z}\text{Co}_z)\text{O}_3$  system under the magnetic fields of (a) 0 T and (b) 5 T. The closed symbols denote  $T_c$  and the open symbols denote  $T_{CO}$  or  $T_N$ . The determination methods of the phase diagram are explained in the text.

anomaly in the heating run for all the samples. In Fig. 5(a), FM-M state appears in the Ca concentration range between  $X=0.35$  and  $0.45$ .  $T_c$ - $X$  curve shows a moderate maximum at around  $X=0.40$ .  $T_c$  decreases with increasing  $Z$  and then vanishes for the  $Z=0.10$  samples. In the CO (AFM-I) region,  $T_{CO}$  decreases with increasing  $Z$  monotonically and then becomes obscured for the  $Z=0.10$  samples. In the case of the applied field of 5 T in Fig. 5(b), the FM-M region is expanded and the  $X$  dependence of  $T_c$  is emphasized.  $T_c$  of the  $Z=0.02\sim 0.06$  samples shows a maximum at around  $X=0.45$ , shifting to higher  $X$  than that at 0 T. The magnetic field surely suppresses CO, but its enhancing effect on the FM-M order is more conspicuous.

Finally, we compare the effect of the Co doping with that of other transition metal doping. Figure 6 shows  $\rho(T)$  of  $\text{Pr}_{0.65}\text{Ca}_{0.35}(\text{Mn}_{0.96}\text{M}_{0.04})\text{O}_3$  ( $M=\text{Co}, \text{Cr}, \text{Ni}$ ) samples. The  $\rho(T)$  curves for the Cr- and Ni-doped samples are almost indistinguishable and the transitions to the FM-M phase are rather gradual. In contrast, the Co-doped sample shows a very sharp first-order-like FM-M transition. The first-order-like and second-order-like FM-M transitions have also been confirmed by the  $M(T)$  measurements for respective samples. Katsufuji *et al.*<sup>7)</sup> observed qualitatively very similar phase diagram

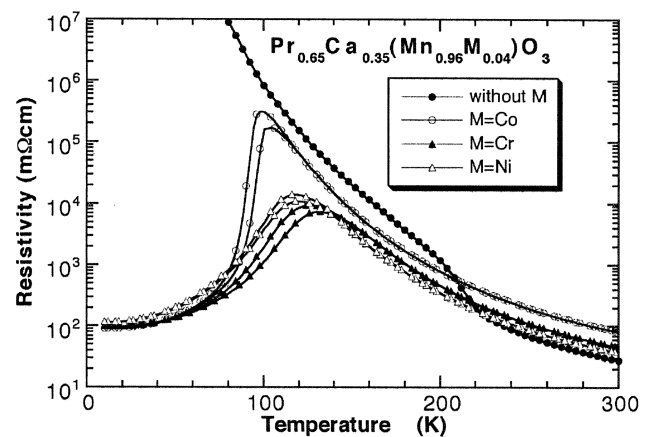


Fig. 6. The temperature dependence of the electrical resistivity  $\rho(T)$  of  $\text{Pr}_{0.65}\text{Ca}_{0.35}(\text{Mn}_{0.96}\text{M}_{0.04})\text{O}_3$  ( $M=\text{Co}, \text{Cr}, \text{Ni}$ ) samples.

for  $\text{Pr}_{1-x}\text{Ca}_x(\text{Mn}_{0.97}\text{Cr}_{0.03})\text{O}_3$  as the present Co-doped system. They suggested from the electron microscope analyses that the long-range CO rapidly gave place to the short-range one by addition of a small amount of Cr impurities.  $\rho(T)$  in Fig. 6 supports that the Ni impurity behaves very similarly to Cr. The results in Fig. 6 also suggest that the long-range CO is somewhat more tough against Co impurities. This quantitative difference in the behavior of Co and Cr (and Ni) impurities may be related to the different 3d electron configuration of each ion. In order to elucidate the origin of the difference, more detailed information is necessary. Further investigations on this theme are under way.

#### §4. Summary

On the basis of the magnetization  $M(T)$  and the electrical resistivity  $\rho(T)$  measurements, the magnetic and electronic phase diagram of  $\text{Pr}_{1-x}\text{Ca}_x(\text{Mn}_{1-z}\text{Co}_z)\text{O}_3$  system was proposed as a function of Ca and Co concentrations  $0.20 \leq X \leq 0.80$ ,  $Z=0\sim 0.10$  under the magnetic fields of 0 T and 5 T. Similarly to the Cr-substituted system, the ferromagnetic metallic (FM-M) state which had been masked out by the charge/orbital order appeared by the Co substitution and/or by applying the high magnetic field. By comparing with the cases of the Cr- and Ni-substitution, the charge/orbital order suppressing effect is somewhat weaker for the Co-substitution case.

- 1) Y. Tokura, A. Urushibara, Y. Moritomo, T. Arima, A. Asamitsu, G. Kido and N. Furukawa: J. Phys. Soc. Jpn. **63** (1994) 3931.
- 2) S. Jin, T.H. Tiefel, M. McCormack, R.A. Fastnacht, R. Ramesh and L.H. Chen: Science **264** (1994) 431.
- 3) Z. Jirak, S. Krupicka, Z. Simsa, M. Dlouha and S. Vratilav: J. Mag. Mag. Mat. **53** (1985) 153.
- 4) B. Raveau, A. Maignan and C. Martin: J. Solid State Chem. **130** (1997) 162.
- 5) F. Damay, A. Maignan, C. Martin and B. Reveau: J. Appl. Phys. **82** (1997) 1485.
- 6) H. Fujishiro, S. Kanoh, H. Yamazaki and M. Ikebe: to be published in J. Phys. Soc. Jpn. **70** (2001).
- 7) T. Katsufuji, S-W. Cheong, S. Mori and C-H. Chen: J. Phys. Soc. Jpn. **68** (1999) 1090.